

## From dust to dose: Effects of forest disturbance on increased inhalation exposure

Jeffrey J. Whicker<sup>a,b,\*</sup>, John E. Pinder III<sup>b</sup>, David D. Breshears<sup>c</sup>, Craig F. Eberhart<sup>a</sup>

<sup>a</sup> Los Alamos National Laboratory, Health Physics Measurements Group, Mail Stop J573, Los Alamos NM 87545, United States

<sup>b</sup> Colorado State University, Department of Environmental and Radiological Health Sciences, Ft. Collins CO 80523, United States

<sup>c</sup> University of Arizona, School of Natural Resources, Institute for the Study of Planet Earth, and Department of Ecology and Evolutionary Biology, Biological Sciences East 325, 1311 E Fourth Street, P.O. Box 210043, Tucson AZ 85721-0043, United States

Received 14 October 2005; received in revised form 3 March 2006; accepted 6 March 2006

Available online 17 April 2006

### Abstract

Ecosystem disturbances that remove vegetation and disturb surface soils are major causes of excessive soil erosion and can result in accelerated transport of soils contaminated with hazardous materials. Accelerated wind erosion in disturbed lands that are contaminated is of particular concern because of potential increased inhalation exposure, yet measurements regarding these relationships are lacking. The importance of this was highlighted when, in May of 2000, the Cerro Grande fire burned over roughly 30% of Los Alamos National Laboratory (LANL), mostly in ponderosa pine (*Pinus ponderosa*) forest, and through areas with soils containing contaminants, particularly excess depleted and natural uranium. Additionally, post-fire thinning was performed in burned and unburned forests on about 25% of LANL land. The first goal of this study was to assess the potential for increased inhalation dose from uranium contaminated soils via wind-driven resuspension of soil following the Cerro Grande Fire and subsequent forest thinning. This was done through analysis of post-disturbance measurements of uranium air concentrations and their relationships with wind velocity and seasonal vegetation cover. **We found a 14% average increase in uranium air concentrations at LANL perimeter locations after the fire, and the greatest air concentrations occurred during the months of April–June when wind velocities are highest, no snow cover, and low vegetation cover.** The second goal was to develop a methodology to assess the relative contribution of each disturbance type towards increasing public and worker exposure to these resuspended soils. Measurements of wind-driven dust flux in severely burned, moderately burned, thinned, and unburned/unthinned forest areas were used to assess horizontal dust flux (HDF) in these areas. Using empirically derived relationships between measurements of HDF and respirable dust, coupled with onsite uranium soil concentrations, we estimate relative increases in inhalation doses for workers ranging from 15% to 38%. Despite the potential for increased doses resulting from these forest disturbances, the estimated annual dose rate for the public was  $<1 \mu\text{Sv yr}^{-1}$ , which is far below the dose limits for public exposures, and the upper-bound dose rate for a LANL worker was estimated to be  $140 \mu\text{Sv yr}^{-1}$ , far below the  $5 \times 10^4 \mu\text{Sv yr}^{-1}$  occupational dose limit. These results show the importance of ecosystem disturbance in increasing mobility of soil-bound contaminants, which can ultimately increase exposure. However, it is important to investigate the magnitude of the increases when deciding appropriate strategies for management and long-term stewardship of contaminated lands. Published by Elsevier B.V.

**Keywords:** Wind erosion; Environmental disturbance; Dust; Uranium; Environmental contaminants

\* Corresponding author. Los Alamos National Laboratory, Health Physics Measurements Group, Mail Stop J573, Los Alamos NM 87545, United States. Tel.: +1 505 667 2610; fax: +1 505 665 7686.

E-mail address: [jjwhicker@lanl.gov](mailto:jjwhicker@lanl.gov) (J.J. Whicker).

## 1. Introduction

Processes driving wind erosion and transport of soil and associated contaminants are of central concern for a diverse set of issues including ecosystem management and risk assessment (NAS, 1989; Toy et al., 2002; Breshears et al., 2003). Loss and redistribution of soil and associated contaminants by wind erosion can result in significant short- and long-term effects on human and ecosystem health (Saxton, 1995; Ludwig et al., 1997; Griffin et al., 2001). Ecological and human risks associated with wind-driven transport of environmental contaminants might be amplified after environmental disturbances through reductions in vegetation cover and disturbance in soil surfaces (Fryrear, 1985; Whitford et al., 1998; Grantham et al., 2001; Kaiser, 2004). While wind erosion processes have been studied extensively in agricultural and desert environments, rates of wind erosion and transport of soils have been made in few other ecosystems despite studies that show wind-driven mechanisms are a critical pathway for contaminant transport (Whicker and Shultz, 1982; Breshears et al., 2003). Further, studies directly linking measured rates of wind erosion directly to particle-size dependencies, as needed to quantify inhalation risk from exposure to environmental contaminants attached to dust, are lacking in both undisturbed and disturbed ecosystems.

The few studies that have measured rates of wind erosion in systems other than agricultural fields, desert ecosystems, or other generally vegetation free surfaces suggest that wind erosion processes drive a substantial fraction of total soil transport at a site, though most studies have focused on water erosion (Breshears et al., 2003). Indeed, rates of soil transport by wind are relatively large not only in arid ecosystems, where such a differences might be expected, but also in semiarid forests, where it is probably not expected (Breshears et al., 2003).

Of additional concern are the implications of vegetation dynamics for contaminant transport and associated risk. Most risk assessments assume static conditions for vegetation and associated ground cover, yet climate or management can drive major changes in vegetation. For example, semiarid forests can change rapidly in response to climate-induced drought or fire (Allen and Breshears, 1998; Breshears and Allen, 2002) and to forest management that implements tree thinning, which is a major strategy for reducing fire risk (Friederici, 2003). Not surprisingly, wind erosion may increase in response to such changes in forests (Whicker et al., 2005, 2006), as has also been shown for shrub lands and rangelands (Zobeck et al., 1989; Whicker et

al., 2002). Hence, risks associated with the environmental transport of contaminants by wind may be greater than previously appreciated in semiarid environments, particularly in forest ecosystems, and particularly in disturbed forests.

Here we evaluate the potential for wildfire and tree thinning to increase transport rates of environmental contaminants driven by wind. Our study focuses on the implications for particle-size dependent contaminant transport for semiarid forest that is undisturbed or that is disturbed as a result of fire or thinning. We evaluated this issue at a site where contaminant transport is of concern: Los Alamos National Laboratory (LANL) — a U.S. Department of Energy Facility located in northern New Mexico. Various radioactive and chemical contaminants have been deposited onto surface soils at LANL as a result of operations over the past several decades (Fresquez et al., 1998). Of particular concern is uranium. Uranium is both a radiological and toxicological hazard and, while naturally occurring, relative large amounts are used in explosives testing at LANL (LANL, 2002), but is also used more broadly for other military purposes, particularly depleted uranium, due to its high density (Guilmette et al., 2004). These activities have resulted in scattering excess uranium into the environment where generally it is eventually deposited onto soil surfaces.

The potential for wind-driven transport of this deposited uranium has been an issue of concern for LANL, and the concern became elevated after a wildfire burned about 3000 ha of ponderosa pine forests across LANL in 2000 (LANL, 2000; Whicker et al., 2006). Fire risk remained high for many areas after the fire, and hence LANL conducted extensive forest tree thinning operations to reduce additional fire risk (LANL, 2001). Although not quantified at the time, such operations might be expected to also increase wind erosion (Whicker et al., 2005), and evidence of low, but elevated, uranium air concentrations after the fire prompted additional interest (Kraig et al., 2001; LANL, 2002).

The motivations for this study were to investigate unanswered questions regarding 1) the general role of wind-driven resuspension of soil-bound contaminants at LANL, 2) the impact of the forest disturbance toward increasing wind-driven resuspension of these contaminants, and 3) the level of potential increases in exposure to contaminated airborne dust for LANL outdoor field workers whose job sites may be near the dust source areas, but in areas not monitored because the dose levels are expected to be low. Hence, an integration of field-based measurements of dust flux, particle size dependencies, and site-specific concentrations is needed for

specific assessments at LANL as a demonstrated approach that could be applied.

The specific goals of this study were to 1) assess the overall potential for wind-driven resuspension of contaminated soil in a forest ecosystem as an exposure pathway for workers and the public, 2) develop a methodology combining dust flux measurements made in disturbed forested areas at LANL with measurements of respirable dust to quantify potential increases in resuspension and inhalation of uranium and for other contaminants of concern, and 3) demonstrate a qualitative method to assess the relative impacts of forest fire and tree thinning on offsite exposures. Hence, we obtained measurements related to wind-driven transport and associated particle-size dependent implications for undisturbed and disturbed semiarid forest to simultaneously aid site-specific risk assessment and address the broader issue of risk implications associated with ecosystem disturbance.

## 2. Methods

### 2.1. Site description

The location of the study was along the western edge of LANL property located about 2–3 km southwest of Los Alamos, NM, USA (35°52'N and 106°19'W) and just east of New Mexico Highway 501 at an elevation of about 2400 m (Fig. 1). The pre-fire vegetation was dominated by *Pinus ponderosa* Douglas ex P. and *C. Lawson* var. *scopulorum* Englem (ponderosa pine) and a variety of grasses and flowering plants (Fox and Hoard, 1995). Because of access restrictions, the areas used in this study did not contain notable levels of contaminants, but the study sites were within a few km of contaminated sites and had similar vegetation, soil, topography, and geology.

Within each of the disturbed and undisturbed forest categories, two sampling plots, a primary and secondary site, were selected to assess variability within each category (Fig. 1). A line transect was established in each of the sampling areas along which the dust sampling stations were positioned every 30 m. This dust sampling transect consisted of three dust sampling stations in the primary sampling sites and two in the secondary sampling sites. In addition to sampling locations in the disturbed and undisturbed areas, various dust samplers were also set up at a fourth site that was adjacent the TA-6 meteorological tower operated by LANL (Rishel et al., 2003) and used for assessment of relationships between saltating dust flux and respirable dust concentrations. This meteorological tower was within several km of all

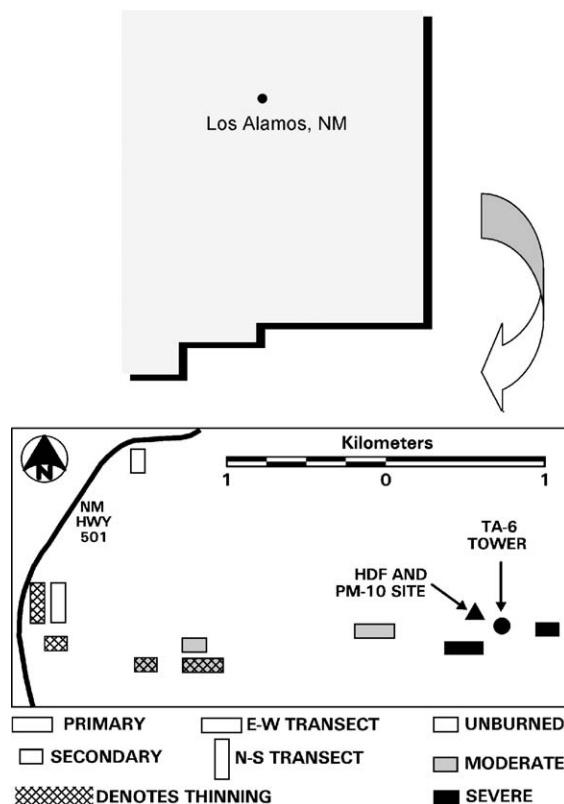


Fig. 1. Location of sampling plots relative to the state of New Mexico, city of Los Alamos, and New Mexico Highway 501, which borders the west side of LANL. The burn gradient is represented as variously shaded boxes. Within each burn category, the Primary sampling sites are represented as larger rectangles and Secondary sites represented as smaller rectangles. Thinned sites are represented with cross-hatching. The map also shows the locations of the TA-6 meteorological tower and the sites used to establish relationships between HDF and PM-10 measurements.

the sampling sites and had the electrical power necessary to power sampling pumps for air sampling.

#### 2.1.1. Burned areas

The Cerro Grande fire burned over approximately 3000 ha of LANL property and was primarily contained in the ponderosa pine forests along the western part of LANL and within canyon bottoms (LANL, 2000). The severity of the burning varied from low- and moderate-burn intensity ground fires to high-burn intensity crown fires. As part of the overall study, measurements of dust flux were made at sites in three categories of burn severity, which were established to assess dust flux along a burn gradient (Whicker et al., 2006). First, severely burned sites were characterized as having ground vegetation and litter cover consumed in the fire and all portions of the pine trees burned, including the

crown (tree top). Second, moderately burned sites included areas where the fire was primarily a ground fire that consumed the vegetation and litter cover but did not reach the top crown of the pine trees. Most trees in the moderately burned areas contained green needles in at least the top third of the tree. The third forest sites were unburned and used as comparison sites.

### 2.1.2. Tree-thinned areas

To reduce the potential for future fire damage to nuclear facilities and to improve the forest “health” (Covington, 2003; Mast, 2003), tree thinning was planned for large areas within LANL boundaries for the years 2001–2003, with the main focus of the tree thinning done in unburned and burned ponderosa pine forest (LANL, 2001). Because of the large amount of land needing thinning, mechanized techniques were used including the use of track-mounted feller bunchers (manufactured by Timbco), skidders, stroke delimiters, and logging trucks to haul off the lumber (Quam L, personal communications, 2004). Thinning reduced tree densities in the ponderosa pine forest by 32% to 86% and also exposed approximately 20% bare soil in the thinned areas (Buckley et al., 2003; Whicker et al., 2005).

### 2.2. Determining the role of wind-driven resuspension for offsite dose

Public radiation doses from inhalation of various radionuclides are assessed through measurements of air concentrations of a variety of radionuclides at approximately 50 locations in and around LANL, as part of the “AIRNET” air-sampling network (LANL, 2002). These measurements include  $^{238}\text{U}$ , the predominant radioisotope of the forms of uranium (>99%) used at LANL. The primary mechanism for inhalation exposure to  $^{238}\text{U}$  from LANL sources is suspected to be through wind-driven resuspension of contaminated soils on LANL property. If true, one would expect the highest concentrations of  $^{238}\text{U}$ , from LANL or non-LANL sources, during the spring months, which in Los Alamos are the windiest (Bowen, 1990) and vegetation the lowest (Pinder et al., 2004). Therefore, measurements made through the LANL air sampling network AIRNET were used to investigate the exposure scenario of wind-driven resuspension through 1) temporal analysis of the  $^{238}\text{U}$  concentrations for a 10-year period, 2) statistical comparisons of the concentrations by quarter, and 3) investigation of the seasonal relationships between  $^{238}\text{U}$  concentration, wind velocity, and vegetation cover. Further, the

potential impact of the Cerro Grande fire and subsequent forest thinning on  $^{238}\text{U}$  concentrations was investigated by statistically comparing pre- and post-fire air concentrations using the non-parametric Mann–Whitney test (Mostteller and Rourke, 1973).

### 2.3. Calculations for potential dose to LANL workers

Because air sample measurements of PM-10 (particulate matter less than 10  $\mu\text{m}$  in aerodynamic diameter) aerosol in each disturbed forest location were not feasible in these remote locations, a correlation between dust flux and PM-10 concentrations was needed to estimate potential doses as impacted by forest fire and thinning. Therefore, side-by-side measurements of horizontal dust flux (HDF) and concentrations of PM-10 measurements were made at an analog site located near the TA-6 meteorological site (Fig. 1) and correlated. Estimates of potential dose for a LANL worker from being in the disturbed areas were made based on this relationship. Though PM-10 measurements were used to calculate doses, Department of Energy (DOE) regulations require making a conservative (i.e., resulting in a higher dose estimate) assumption that all inhaled dust consisted of particles with 1  $\mu\text{m}$  aerodynamic diameters (DOE, 1993), which was done for this study.

#### 2.3.1. Correlation of horizontal dust flux and PM-10 concentration measurements

HDF was measured using Big Spring Number Eight (BSNE) samplers (Fryrear, 1986). These passive samplers self-orient a 10  $\text{cm}^2$  opening into the wind through which airborne dust is carried into in a horizontal direction, decelerated, and deposited into a collection pan. These BSNE field dust collectors have been extensively tested and show good sampling efficiency for soils with higher fractions of sand and silt (Fryrear, 1986; Goossens and Offer, 2000), which are abundant at LANL (Nyhan et al., 1978). Importantly, BSNE samplers do not require electricity, which permits use in remote locations. The HDF was calculated as the collected mass divided by the product of the sampler opening (10  $\text{cm}^2$ ) and the sampling period and is expressed in units of  $\text{g m}^{-2} \text{d}^{-1}$ .

To establish relationships between HDF measurements and exposure-related metrics, the correlation between average HDF measured at 1 m above the ground and PM-10 concentration measurements was needed. A TEOM (Tapered Element Oscillating Microbalance) Series 1400a Ambient Particulate Monitor was used to continuously measure PM-10 concentrations in

0.5 h increments. The sampler is manufactured by Ruprecht and Pataschnick Co., Inc of Albany, New York. It has been designated as a U.S. EPA equivalent method for the determination of 24-h average PM-10 concentrations in ambient air. A size selective inlet uses impaction to achieve a 50% particle collection cut point of about 10  $\mu\text{m}$  at a flow rate of  $1.67 \times 10^{-2} \text{ m}^3 \text{ min}^{-1}$ . A portion of this flow,  $3 \times 10^{-3} \text{ m}^3 \text{ min}^{-1}$ , goes through a filter that is fixed to the free end of a tapered oscillating “finger” or element. Mass changes on the filter, measured by changes in the vibration frequency, are used to calculate air concentrations.

TEOM measurements were conducted from 28 June 2001 to 23 July 2002 at the TA-6 meteorological station. Though some data were lost due to disruptions in electrical power, approximately 14,350 30-min mass concentration means were recorded. Some of these data were discarded due to low flow rates and pronounced negative values  $< -2 \mu\text{g m}^{-3}$  were discarded. A total of 14,007 measures from 313 days were obtained.

Daily means were computed by averaging the 30-min means, and daily means were retained in the data when  $\geq 36$  30-min intervals were available for a given day. Daily means were available for 290 days with 97% of these days having measures from  $> 44$  30-min intervals. Averages of TEOM daily means were computed for sampling intervals of the BSNE data collected from the TA-6 meteorological location and compared to mean HDF measures at a 1-m sampling height for the same sampling interval. Because of the considerable day-to-day variability observed in TEOM data, only those intervals of longer than 10 days where TEOM data were available from  $> 50\%$  of the days were involved in these comparisons.

### 2.3.2. Procedure for calculating potential dose and assumptions

A linear-least squares regression was performed with the PM-10 concentrations from TEOM measurements ( $C_{\text{PM-10}}$ ) as the dependent variable and the mean of the 1-m HDF measurements made at the adjacent BSNE sampler locations as the independent variable. The general form of this linear model of this relationship was:

$$C_{\text{PM-10}} = (\text{HDF})(m) + b \quad (1)$$

where  $m$  and  $b$  are the best fit slope and intercept of the equation, respectively. The slope,  $m$ , represents the effectiveness of saltating particles to suspend PM-10 particles and the intercept,  $b$ , represents an average “background” PM-10 concentration.

An important assumption is that the relationship in Eq. (1) holds in other sampling locations. Because of limitations in access to electrical power, we were not able to fully test this relationship at all sites. Fundamentally though, BSNE samplers almost exclusively measure wind-blown saltating soil particles (Fryrear, 1986), and the impaction of the saltating particles onto the soil surface is the main mechanism for suspension of smaller soil particles (Bagnold, 1941). Therefore, for these calculations, we assume a similar relationship between HDF and  $C_{\text{PM-10}}$  concentrations at other sites, though recognizing the uncertainty. We expect that this relationship, because it was made in an open grassy area of forest, would be steeper than one in a forested area with greater ground cover because the measured HDF in the unburned forests would reflect more background dust relative to saltating particles (Whicker et al., 2006).

### 2.3.3. Calculation of expected and upper-bound uranium inhalation dose for LANL workers

Because of the focus on LANL workers, the following inhalation dose calculations are based on exposure parameters for occupational workers and use generally conservative assumptions to estimate an average and an upper bound of potential dose. The dose estimates are based on the empirical model describing the relationship between the mean HDF in each of the disturbed forest location and the  $C_{\text{PM-10}}$  concentration and the following assumptions: 1) calculations are based on onsite uranium soil concentrations, with an average of  $0.25 \text{ Bq g}^{-1}$  and an onsite average+2 standard deviations of  $0.50 \text{ Bq g}^{-1}$  (both values from LANL (2002)), and high-end mean uranium concentration in LANL soils as measured at the EF firing site of  $116.9 \text{ Bq g}^{-1}$ , 2) a conservative enrichment of 5 times the concentration of uranium in the PM-10 aerosol relative to the soil (Shinn et al., 1997; Van Pelt and Zobeck, in press), 3) exposure scenarios that outdoor workers either work at all burn and thinned locations equally through the year (used average and average+2 std soil concentrations) or at a single highly contaminated disturbed site (used measured soil concentrations of uranium from EF firing site), and 4) the workers spend their entire work year outdoors (no shelter) in the location(s).

The first step in this dose assessment is to convert  $C_{\text{PM-10}}$  to an activity concentration for uranium ( $C_{\text{U-PM-10}}$ ) in units of  $\text{Bq m}^{-3}$ . To convert, we multiply  $C_{\text{PM-10}}$  (units of  $\text{g}_{\text{soil}} \text{ m}^{-3}$ ) with the soil concentration measurements from soil collected in the top 5 cm of soil on LANL property ( $C_{\text{soil}}$ —units of  $\text{g}_{\text{U}} \text{ g}_{\text{soil}}^{-1}$ ), the

enrichment ratio (ER), and the specific activity of uranium ( $SA_U$ ) in units of  $Bq\ g_u^{-1}$  (Eq. (2)).

$$C_{U-PM-10} \frac{Bq_U}{m^3} = C_{PM-10} \times C_{soil} \times ER \times SA_U \quad (2)$$

The average onsite uranium concentration value ( $C_{soil}$ ) was  $3.6 \times 10^{-6}$  g of uranium per gram of surface soil and an upper-bound concentration (2 standard deviations above the mean) of roughly  $7.2 \times 10^{-6}$  g of uranium per gram of soil (LANL, 2002). An upper-bound estimate of soil concentration at a firing site was  $1.67 \times 10^{-3}$   $g_u\ g_{soil}^{-1}$ . Because most of the uranium used at LANL was in the depleted form, for these calculations we assume that the uranium in the soil has a specific activity ( $SA_U$ ) of 14,000  $Bq\ g_u^{-1}$  (Guilmette et al., 2004) and an ER of 5.

Next, the link between HDF and  $C_{PM-10}$  was used to estimate potential increases in doses from inhaled uranium. The doses to workers are calculated using Derived Air Concentrations (DAC) listed in DOE (1993). The DAC values represent air concentrations of 1  $\mu m$  diameter particles that if inhaled by a worker for 40 h per week, 50 weeks of the year (for a total respired volume of 2400  $m^3$ ) the worker would receive a 50 mSv committed effective dose equivalent (CEDE), or the DOE occupational dose limit (DOE, 1993). The DAC value for  $^{238}U$  (the dominant isotope of uranium) is listed as 0.6  $Bq\ m^{-3}$  for class Y lung solubility (to estimate maximum radiation dose). The estimated doses then become:

$$\text{Dose (mSv)} = C_{U-PM-10} \times \frac{50\ \text{mSv}}{0.6\ \frac{Bq}{m^3}} \quad (3)$$

#### 2.4. Quantification of relative impact of forest disturbances on uranium air concentrations

Using the empirical model shown in Eq. (1) and its conversion shown in Eq. (2), the fractional increases in  $C_{U-PM-10}$  ( $RI_i$ ) for each disturbance type ( $i$ ) in each of the disturbed areas compared to the undisturbed forest can be calculated by ratio. These ratios can then be used in combination with the relative area for each disturbance ( $FA_i$ ) to estimate the percent increase in  $C_{U-PM-10}$  concentrations across the LANL when summed over all disturbance types (Eq. (4)).

$$\% \text{ Increase} = \sum_i FA_i \times RI_i \times 100\% \quad (4)$$

As shown in Eq. (4), the fractional amounts of burned, unburned, and thinned areas ( $FA_i$ ) were needed to estimate the increase in  $C_{U-PM-10}$  dust across the

LANL site as a result of these forest disturbances. An estimated 25% (~ 2800 ha) of LANL area was thinned following the Cerro Grande (Smith, S—personal communication, 2005), but assessment of the area of burned and unburned forest area was more difficult. Because the classifications of fire severity as severe and moderate can vary among agencies and individuals, the extent of the Severe and Moderate burn categories as used in this study was estimated by comparing pre-fire and post-fire Thematic Mapper (hereafter, TM) satellite images. These TM images contain 6 bands of reflected electromagnetic radiation in the visible and infrared bands that are recorded from 30 by 30-m areas termed pixels (Lillesand and Kiefer, 1994). Pre-fire and post-fire images were obtained for the dates of March 13, 2000 and April 1, 2001, respectively, and rectified to NAD-27 Universal Transverse Mercator coordinates (Lillesand and Kiefer, 1994). These late-winter and early-spring images were used to 1) insure the absence of snow cover, whose highly-reflective surface can complicate the interpretation of vegetation patterns, and 2) predate the onset of seasonal, herbaceous plant growth. Extensive herbaceous growth promoted by post-fire remediation efforts could complicate the assessment of damage to pine tree canopies.

To assess damage to pine canopies, the data in the TM images were converted to Normalized Difference Vegetation Indices (hereafter, NDVI; Lillesand and Kiefer, 1994), which are a measure of chlorophyll abundance based on ratios of infrared to visible reflectance. A reduction in NDVI between the pre-fire and post-fire images for a pixel is an indication of chlorophyll loss and fire damage to the canopy within that pixel. The degree of this difference for pixels was scaled to be representative of that for plots of Severe and Moderate fire severity. Pixels were scored as Severe burn when there were pine canopies present before the fire but no evidence of live trees after the fire. Pixels were scored as Moderate burn when there was at least some evidence of live trees after the fire. Pixels where there was little difference between pre- and post-fire NDVI were scored as unburned. However, low intensity ground fires that caused little scorching or mortality of large pines would 1) not have caused a measurable change in NDVI and 2) would not be detected by this procedure.

Because the pre-fire, late-winter image was unsuitable for mapping land cover types, land cover maps developed in the Multiple Resolution Land Cover program (Vogelmann et al., 1998) were used to show the extent of ponderosa pines, piñon/juniper, shrub land and grassland vegetation on LANL.

### 3. Results

#### 3.1. Role of wind-driven resuspension toward public exposure

The air concentrations of  $^{238}\text{U}$  from 1995 to 2005 measured by the AIRNET air sampling network are plotted in Fig. 2a and show a seasonal pattern with the highest concentrations generally found in the second quarter (April–June) of each year as shown in Fig. 2b. A Mann–Whitney rank sum test was used to compare  $^{238}\text{U}$  concentrations among the sampling quarters and showed that the concentrations were statistically higher in the second quarter relative to the other three quarters ( $P < 0.05$ ), with the other three quarters not being significantly different from each other. Wind velocities are generally greater during the second quarter (Bowen,

1990), and we found that the  $^{238}\text{U}$  concentrations in air are significantly correlated to the average gust wind velocity (Fig. 3). Increased wind velocities, combined with lower vegetation in the early spring (Pinder et al., 2004), are likely factors in the increased  $^{238}\text{U}$  concentrations in the second quarter. In addition, we found that the  $^{238}\text{U}$  concentrations, when averaged across all LANL AIRNET monitoring sites, have increased significantly ( $P < 0.05$ ) by about 14% since the Cerro Grande fire (Fig. 4).

#### 3.2. Calculations for potential dose to LANL workers

##### 3.2.1. Correlation between HDF and PM-10 concentration

The average HDF measurement at the HDF/PM-10 location at TA-6 (Fig. 1) was  $1.05 \text{ g m}^{-2} \text{ d}^{-1}$

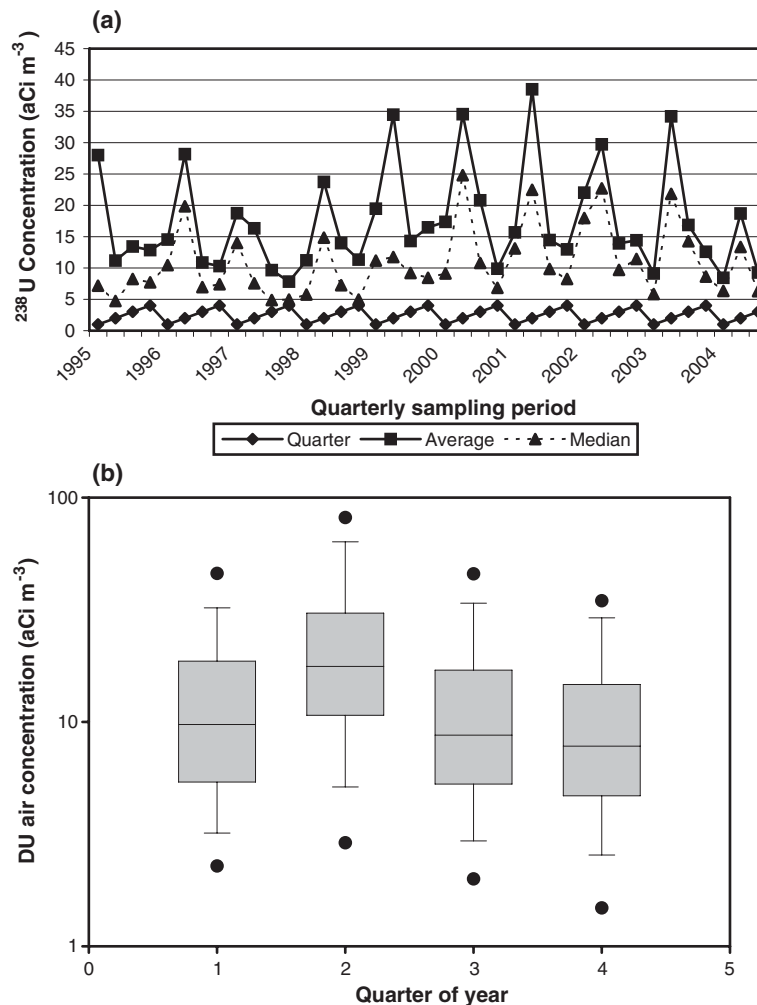


Fig. 2. Plots of quarterly  $^{238}\text{U}$  concentration with time from 1995 through the 3rd quarter in 2004 (a), and the distributions of  $^{238}\text{U}$  concentrations by quarter (b).

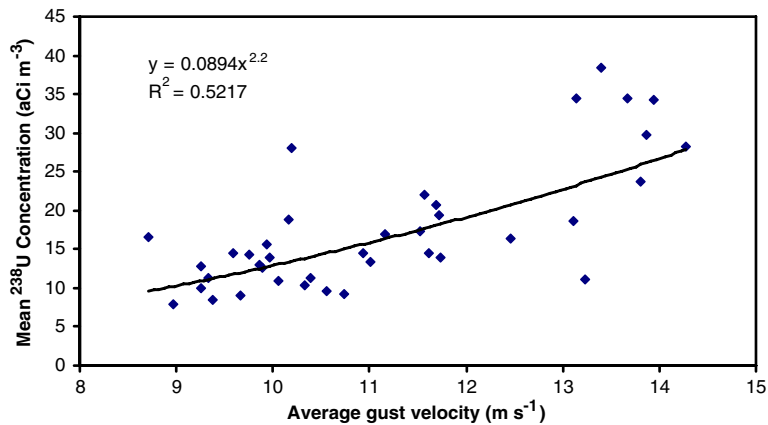


Fig. 3. Relationship of quarterly  $^{238}\text{U}$  concentrations with peak wind velocities and expressed as a power function.

(median =  $0.74 \text{ g m}^{-2} \text{ d}^{-1}$ ) with a standard deviation of  $0.75 \text{ g m}^{-2} \text{ d}^{-1}$  (range from 0.27 up to  $2.46 \text{ g m}^{-2} \text{ d}^{-1}$ ). The average  $C_{\text{PM-10}}$  was  $13.1 \mu\text{g m}^{-3}$  (median =  $11.9 \mu\text{g m}^{-3}$ ) with a standard deviation of  $3.7 \mu\text{g m}^{-3}$  and a range of  $7.94 \mu\text{g m}^{-3}$  up to a maximum of  $20.6 \mu\text{g m}^{-3}$ . The average 1-m HDF measurements made in the burned, thinned, and undisturbed (unburned and unthinned) locations were provided in Whicker et al. (2005, 2006) and are listed in the first row in Table 1.

Using mean HDF and the  $C_{\text{PM-10}}$  measurements from the TA-6 location from overlapping periods, we found a significant correlation between the HDF measurements and mean  $C_{\text{PM-10}}$  measured by a TEOM (Fig. 5). The  $C_{\text{PM-10}}$  measures increased in a statistically significant ( $n=10$ ;  $R^2=0.80$ ;  $P<0.001$ ) linear fashion with increasing mean HDF. The regression equation of  $C_{\text{PM-10}}$  measures on HDF measures has intercept ( $\pm\text{SE}$ ) and slope ( $\pm\text{SE}$ ) of  $8.4 (\pm 1.0)$  and  $4.4 (\pm 0.8)$ , respectively.

$$C_{\text{PM-10}} = \overline{\text{HDF}}(4.4) + 8.4 \quad (5)$$

An analogous regression procedure using the individual daily means of  $C_{\text{PM-10}}$  data rather than the interval mean

also indicated a statistically significant relationship of  $C_{\text{PM-10}}$  to HDF ( $F=63.8$ ;  $df=1, 178$ ;  $P<0.001$ ) with no significant residual relationship due to the sampling intervals (Lack of Fit  $F$ -test = 1.45;  $df=8, 170$ ;  $P>0.05$ ). The intercepts and slopes of this procedure were similar to those in Eq. (5).

### 3.2.2. Increases in $C_{\text{PM-10}}$ and $C_{\text{U-PM-10}}$

Forest disturbance increased the mean HDF by 49%, 222%, and 72% in the moderately burned, severely burned, and thinned areas, respectively. Next, the empirical relationship shown in Eq. (3) was used to

Table 1

Summary of results and calculations for increases in PM-10 concentrations in each of the burn/unburn categories

	Unburned	Moderately burned	Severely burned	Thinned
Mean HDF ( $\text{g m}^{-2} \text{ d}^{-1}$ )	0.85	1.27	1.89	1.46
PM-10 concentration ( $\mu\text{g m}^{-3}$ )	12.16	14.02	16.72	14.84
Relative PM-10 conc. in burned forests relative to unburned	1.00	1.15	1.38	1.22
Est. fraction of burned/unburned areas LANL				0.35
NDVI data	0.96	0.03	0.01	
LANL (2001) data (low burn = mod. burn)	0.69	0.30	0.01	
Overall weighted average increase in PM-10 from fire and thinning	Burn contribution			
	1.00 (0.96) + 1.15 (0.03) + 1.38 (0.01) = 1.01 (NDVI data)			
	1.00 (0.69) + 1.15 (0.30) + 1.38 (0.01) = 1.05 (LANL, 2001 data — low burn = mod. burn)			
	Thinning contribution			
	1.00 (0.75) + 1.22 (0.25) = 1.06			

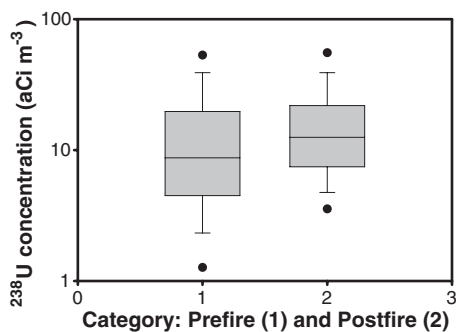


Fig. 4. Pre- and post-fire distribution of quarterly  $^{238}\text{U}$  concentrations.



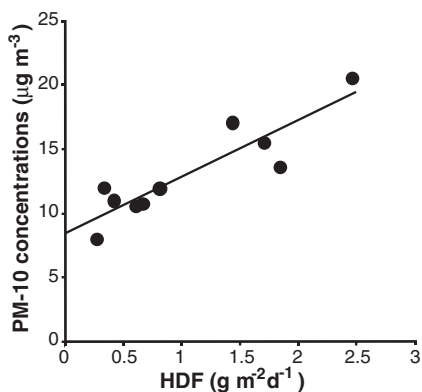


Fig. 5. PM-10 concentrations as related to HDF measurements. The estimated intercept for the regression is  $8.4 \pm 1.0$  with a slope of  $4.4 \pm 0.8$ . The coefficient of determination is 0.80.

estimate mean  $C_{\text{PM-10}}$  for each of the disturbed areas using the HDF measurements from the disturbed and undisturbed areas. We estimated a 15% increase in  $C_{\text{PM-10}}$  in the moderately burned areas, a 38% increase in the severely burned areas, and a 22% increase in the thinned areas (Table 1).

Eq. (2) was used to calculate  $C_{\text{U-PM-10}}$  and the results are shown in Table 2. The estimates in Table 2 are 2 to 23 times greater than the measured uranium air concentrations at Los Alamos that range from  $1.85 \times 10^{-7}$  up to  $1.1 \times 10^{-6}$  Bq  $\text{m}^{-3}$  (LANL, 2002). This comparison shows the approach above is giving reasonable, and perhaps conservative, values for air concentrations.

The summary for average and upper-bound occupational potential radiation doses from inhalation of uranium (calculated using Eq. (3)) is provided in Table 2. These calculations show that the fire potentially increased the radiation doses in the worst case up to

38% in the severely burned areas, but that the mean and mean+2 std doses ( $0.3$  and  $0.6 \mu\text{Sv yr}^{-1}$ ) were still  $\ll 1\%$  of the  $50,000 \mu\text{Sv}$  annual occupational dose limit. The estimated dose rate for the upper-bound exposure scenario at a severely burned site was  $140 \mu\text{Sv yr}^{-1}$ , or about 0.3% of the annual occupational dose limit. In addition, one should consider that field workers do not generally occupy only one area type throughout a year. To account for the exposure scenario where a worker moves through multiple disturbed/undisturbed areas, the dose estimate could be calculated as a weighted average of the dose based on the fraction of time spent in each category of disturbed/undisturbed area.

### 3.3. Quantification of relative impact of forest disturbances on uranium air concentrations

The relative impacts of forest disturbance toward increased uranium air concentrations were assessed using Eq. (4). This calculation requires knowledge of the fractional increase in uranium air concentrations and the fractional area for each disturbance type.

#### 3.3.1. Relative impact of forest fire on uranium air concentrations

The comparison of pre-fire and post-fire NDVIs estimated that severe burns occurred in 127 ha of ponderosa pine and piñon/juniper woodlands and 746 ha of moderate burns occurred on these woodlands. Most of these burns, especially the severe burns, occurred on that portion of LANL south of Los Alamos and in ponderosa pine forests.

The estimate of 873 ha for both Severe and Moderate burns is greater than the 393 ha of “Cerro Grande Fire

Table 2  
Summary of calculation values for estimating doses to occupationally exposed workers from DU contaminated soils

	Unburned	Moderately burned	Severely burned	Thinned
Estimated PM-10 concentration ( $\mu\text{g m}^{-3}$ )	12.16	14.02	16.72	14.84
Estimated DU concentration ( $\text{Bq m}^{-3}$ )				
Mean (+2 std)	$3.1 \times 10^{-6}$ ( $6.1 \times 10^{-6}$ )	$3.5 \times 10^{-6}$ ( $7.1 \times 10^{-6}$ )	$4.2 \times 10^{-6}$ ( $8.4 \times 10^{-6}$ )	$3.7 \times 10^{-6}$ ( $7.48 \times 10^{-6}$ )
Upper-bound	$1.42 \times 10^{-3}$	$1.64 \times 10^{-3}$	$1.95 \times 10^{-3}$	$1.73 \times 10^{-3}$
Estimated dose ( $\mu\text{Sv yr}^{-1}$ )				
Mean (+2 std)	0.22 (0.44)	0.25 (0.51)	0.30 (0.60)	0.27 (0.53)
Upper-bound	102	117	140	124
Net increase above unburned locations ( $\mu\text{Sv yr}^{-1}$ )				
Mean (+2 std)		0.03 (0.07)	0.08 (0.16)	0.05 (0.09)
Upper-bound		15	38	22
Relative increase in dose		15%	38%	22%

High-burn severity” estimated from post-fire TM data by McKown et al. (2003). Because the McKown et al. (2003) study used only post-fire images, their separation between “High-burn severity” and unburned forests probably overlaps the Moderate category used in this study. For example, some areas of moderate burn were not apparent in the April 1, 2000 data and were only identified by comparison of their NDVI to the pre-fire image.

Neither the 873 ha of burned forest estimate or the 393 ha of McKown et al. (2003) are consistent with a previous estimate of 3061 ha of burned area on LANL (LANL, 2001). The 3061 ha estimate includes nonforest areas that burned and forest areas where the fire severity was less than the Moderate burn used here and resulted in too little damage to the pine canopy to be detected from TM data. Low-intensity fires, which consume only a part of the forest floor, can have little effect on the canopies of large trees (Gaines et al., 1958; Davis et al., 1968).

For the purposes of these calculations, we used the NDVI analyses and assumed that of the total 11,694 ha of LANL property a total of 521 ha burned (124 ha was severely burned and the rest, 397 ha, was moderately burned). This gives 3.4% of LANL in the Moderate burned severity class and 1.1% in the Severely burned class. Finally, the last row in Table 1 shows the calculation for an estimated 1% increase of PM-10 concentration across LANL as a result of the fire (Table 1). This value is calculated as the average of increased PM-10 concentrations in the burned areas weighted by the fraction of LANL burned and unburned areas in each of the three burn severity categories. For comparison, we also calculated the increase in PM-10 concentrations using the burn estimates from LANL (2001) which estimated  $2724 \pm 842$  ha of low- to moderate-burn intensity (these were added together into the moderate burn PM-10 category) and 30 ha of severe burn area. These values give an estimated increase of PM-10 aerosol across LANL due to the fire of about 5% (Table 1).

### 3.3.2. Relative impact of forest thinning on uranium air concentrations

Regarding the area for thinning, approximately 2800 ha of the 11,100 ha of LANL property were thinned between the years 2000 and 2003 (Smith, S — personal communication, 2005). This amounts to about 25% of LANL property that was impacted by tree thinning. Using the relationship between HDF and PM-10 concentrations, the relative increase in dust emissions

from post-thinning operations was estimated to be about 6% (Table 1).

## 4. Discussion

This study provides a direct link between increases in horizontal dust flux and respirable dust concentrations. This link is important because the increased HDF in the disturbed forest areas suggests the possibility of increased production of respirable particles in the disturbed areas, some of which contain soils with excess uranium or other contaminants.

The estimates of expected radiation dose rates and plus 2 standard deviations for post-disturbance conditions were greater than those for undisturbed conditions by up to 38%, but even so were small in an absolute sense (e.g.  $< 1 \mu\text{Sv yr}^{-1}$ ) (Table 1), especially relative to the occupational dose limit of  $5 \times 10^4 \mu\text{Sv yr}^{-1}$ . Even the high-end dose rate for a worker working at the EF firing site year round, which if severely burned would have an estimated dose rate of  $140 \mu\text{Sv yr}^{-1}$ , which is still less than 1% of the annual dose limit for an occupational worker (DOE, 1993). These estimated dose rates suggest that while there has likely been a significant increase in uranium concentrations following to the disturbances, the amount of the increase in dose rate, both in worker and public realms, is in the range of other common sources of radiation dose. For example, the maximum estimated dose rate of  $140 \mu\text{Sv yr}^{-1}$  to workers from this study can be compared to the average background dose rate of  $3000 \mu\text{Sv yr}^{-1}$  people receive from natural background sources (e.g., cosmic, terrestrial, radon) and to the  $\sim 30 \mu\text{Sv}$  received from a standard chest X-ray (NCRP, 1987, Wall and Hart, 1997).

While these calculations were performed for uranium, the same approach can be taken for other radioactive and chemical constituents in the resuspendable surface soil as well, though the specific kinetics of the contaminant in the soil may need to be considered (Whicker and Shultz, 1982). For example, using upper soil values of  $9 \times 10^{-3} \text{ Bq g}^{-1}$  of  $^{239}\text{Pu}$  (LANL, 2002), one can calculate an upper-bound annual dose estimate of  $0.37 \mu\text{Sv}$ , assuming 100% of a worker's time is spent in the severely burned area. A total estimated committed effective dose equivalent could also be calculated by summing over doses from all radioactive constituents in the soil. This approach certainly has its limitations due to uncertainty in selection of exposure parameters, but choosing conservative values for dose assessment allows for an initial screening, which if high, would provide the motivation to perform a more thorough evaluation.

#### 4.1. Implications for management and long-term stewardship of contaminated lands

Proper management or remediation of ecosystems often requires direct human intervention to maintain or improve ecosystem function. Prescribed burning and thinning are important management tools to obtain these goals, but these activities on contaminated lands require special precautions and knowledge. The data from this study suggest that these disturbances would likely increase contaminate transport, and the overall increase would depend on the spatial scale and the severity of the disturbance on the cover vegetation. For example, our data suggests that forest fires, especially severe ones, have a greater impact on wind erosion relative to forest thinning, but because thinning was performed over a much larger area than was burned, the overall impact of thinning on dust emissions was greater than the forest fire at LANL.

Further, the methodology outlined also provides an approach to evaluate the effects of future disturbances such as wildfire at LANL. Historically, ponderosa pine forests experienced frequent fires (about 1 every 10 years) that were grass fires of low intensity (Friederici, 2003). In contrast, in the past 50 years there have been 5 major crown fires near LANL that were extensive and resulted in tree mortality over extensive tracts of land (LANL, 2000). In coming years to decades LANL and other semiarid sites will face continuing threats from fire. Because the results of the time-weighted dose calculations are dependent on the amount of area burned and the severity of the burn, hypothetical dose calculations can readily be performed to assess risk consequences from future fires and their associated burn severity.

As for contaminated areas in general, LANL and DOE are faced with decisions regarding clean-up strategies for contaminated sites. One important question to ask about these sites is not how to clean them up, but rather whether or not to clean them up at all (Breshears et al., 1993; Whicker et al., 2004). One of the major clean-up options to be considered—physical removal of the soils—is extremely costly and requires virtual destruction of the contaminated ecosystem (Shinn et al., 1989) and the availability of a new site approved to dispose of the contaminated materials that are removed. Soil substrate removal only translocates the problem, may add significant health risks to the clean-up workers, and may actually enhance the dispersion of contamination in the process (Whicker et al., 2004). In contrast, if the long-term risks from actinides in surface soils of the environment are

sufficiently low, contaminants may be left in place, providing that soil stability, even during extreme disturbance events, is adequately demonstrated.

## 5. Conclusions

This study documents previously unknown relationships between disturbance, dust flux, particle size, and inhalation risk for an extensive type of semiarid forest (ponderosa pine) with an extensive distribution. In a site-specific context, our results indicate minimal dose potential from uranium inhalation for LANL workers, even after disturbance. More generally, however, our results highlight that climate- and management-induced vegetation dynamics can significantly increase dust transport, and that dust transport is directly relevant for estimating health risk.

## Acknowledgements

This work was funded, in part, by the Technology, Development, Enhancement, and Application program at Los Alamos National Laboratory and the remainder was funded by the Department of Energy under contract W7405 ENG-36. The support of Shawna Eisele, Jeffrey Hoffman, Dr. Robert Devine and Dr. Robert Murphy is greatly appreciated. The authors would like to thank Kristine N. Baker for data collection and the following individuals for their invaluable review of this study: Dr. Shawki Ibrahim, Dr. Jeff Collett, Dr. John Zimbrick, and Dr. Ted Zobeck.

## References

- Allen CD, Breshears DD. Drought-induced shift of a forest–woodland ecotone: rapid landscape response to climate variation. *Proc Natl Acad Sci U S A* 1998;95:14839–42.
- Bagdolt RA. The physics of blown sand and desert dunes. London: Chapman and Hall Ltd; 1941. 265 pp.
- Bowen BM. Los Alamos climatology. Los Alamos National Laboratory LA-11735-MS; UC-902. Springfield, VA: National Technical Information Service; 1990.
- Breshears DD, Allen CD. The importance of rapid, disturbance-induced losses in carbon management and sequestration. *Glob Ecol Biogeogr* 2002;11:1–5.
- Breshears DD, Whicker FW, Hakonson TE. Orchestrating environmental research and assessment for remediation. *Ecol Appl* 1993;3:590–4.
- Breshears DD, Whicker JJ, Johansen MP, Pinder JE. Wind and water erosion and transport in semi-arid shrubland, grassland, and forest ecosystems: quantifying dominance of horizontal wind-driven transport. *Earth Surf Processes Landf* 2003;28:1189–209.
- Buckley KJ, Walterscheid JC, Loftin SR, Kuyumjian GA. Final progress report on Los Alamos National Laboratory Cerro Grande fire rehabilitation activities. Los Alamos National Laboratory report LA-UR-03-7139; 2003.

- Covington WW. The evolutionary and historical context. In: Friederici P, editor. *Ecological restoration of southwestern ponderosa pine forests*. Washington, D.C.: Island Press; 2003. p. 26–47.
- Davis JR, Ffolliott PF, Clary WP. A fire prescription for consuming ponderosa pine duff. USDA forest research note RM-115; 1968.
- DOE (Department of Energy). Occupational radiation protection; final rule. Code of Federal Regulations, 10CFR 835; 1993.
- Fox TS, Hoard D. Flowering plants of the southwestern woodlands. Los Alamos, NM: Otowi Crossing Press; 1995. 208 pp.
- Fresquez PR, Armstrong DR, Mullen MA. Radionuclides in soils collected from within and around Los Alamos National Laboratory. *J Environ Sci Health* 1998;A33:263–78.
- Friederici P, editor. *Ecological restoration of southwestern ponderosa pine forests*. Washington, D.C.: Island Press; 2003. 559 pp.
- Fryrear DW. Soil cover and wind erosion. *Trans ASAE* 1985;28:781–4.
- Fryrear DW. A field dust sampler. *J Soil Water Conserv* 1986;41:117–20.
- Gaines EM, Kallendar HR, Wagner JA. Control burning in southwestern ponderosa pines: results from the Blue Mountain plots, Fort Apache Indian Reservation. *J For* 1958;56:323–7.
- Goossens D, Offer ZY. Wind tunnel and field calibration of six aeolian dust samplers. *Atmos Environ* 2000;34:1043–57.
- Grantham WP, Redente EF, Bagley CF, Paschke MW. Tracked vehicle impacts to vegetation structure and soil erodibility. *J Range Manag* 2001;54:711–6.
- Griffin DW, Kellogg CA, Shinn EA. Dust in the wind: long range transport of dust in the atmosphere and its implications for global public and ecosystem health. *Global Change and Human Health* 2001;2:20–33.
- Guilmette RA, Parkhurst MA, Miller G, Hahn FF, Roszell LE, Daxon EG, et al. Human health risk assessment of Capstone depleted uranium aerosols. Attachment 3 of depleted uranium aerosol doses and risk: summary of U.S. assessments. Columbus, OH: Battelle Press; 2004. 350 pp.
- Kaiser J. Wounding earth's fragile skin. *Science* 2004;304:1616–8.
- Kraig D, Ryti R, Katzman D, Buhl T, Gallaher B, Fresquez P. Radiological and nonradiological effects after the Cerro Grande fire. Los Alamos National Laboratory report LA-UR-01-6868; 2001.
- LANL (Los Alamos National Laboratory). A special edition of the SWEIS yearbook: wildfire 2000. Los Alamos National Laboratory report LA-UR-00-3471; 2000.
- LANL (Los Alamos National Laboratory). Wildfire hazard reduction project plan. Los Alamos National Laboratory report LA-UR-2017; 2001.
- LANL (Los Alamos National Laboratory). Environmental surveillance at Los Alamos during 2002. Los Alamos National Laboratory report LA-14086-ENV; 2002.
- Lillesand TM, Kiefer RW. Remote sensing and image interpretation. Third Edition. New York: John Wiley and Sons, Inc.; 1994. 750 pp.
- Ludwig JA, Tongway DJ, Freudenberger DO, Noble JC, Hodgkinson KC, editors. *Landscape ecology, function and management: principles from Australia's rangelands*. Collingwood, Australia: CSIRO Publishing; 1997. 158 pp.
- Mast JN. Tree health and forest structure. In: Friederici P, editor. *Ecological restoration of southwestern ponderosa pine forests*. Washington: Island Press; 2003. p. 215–32.
- McKown B, Koch SW, Balice RG, Neville P. Land cover map for the eastern Jemez Region. Los Alamos National Laboratory report LA-14029; 2003.
- Mosteller F, Rourke F. *Sturdy statistics: nonparametrics and order statistics*. Reading, MA: Addison-Wesley; 1973. 395 pp.
- NAS (National Academy of Sciences-Committee to Provide Interim Oversight of the DOE Nuclear Weapons Complex). *Nuclear weapons complex: management for health, safety and the environment*. Washington, D.C.: National Academies Press; 1989.
- NCRP (National Council on Radiation Protection). *Ionizing radiation exposure of the population of the United States*. National Council on Radiation Protection and Measurements, report, vol. 93; 1987. Washington, D.C.
- Nyhan JW, Hacker LW, Calhoun TE, Young DL. Soil survey of Los Alamos County, New Mexico. Los Alamos Scientific Laboratory report LA-6779-MS; 1978.
- Pinder JE, Whicker JJ, Breshears DD. Effects of the Cerro Grande fire on ponderosa pine forests and recovery of the forest floor at LANL. Los Alamos National Laboratory report LA-UR-04-2495; 2004.
- Rishel JS, Johnson S, Holt D. Meteorological monitoring at Los Alamos. Los Alamos National Laboratory report LA-UR-03-8097; 2003.
- Saxton KE. Wind erosion impacts on off-site air quality in the Columbia Plateau—an integrated research plan. *Trans ASAE* 1995;38:1031–8.
- Shinn JH, Essington EH, Miller FL, O'Farrell TP, Orcutt JA, Romney EM, et al. Results of a cleanup and treatment test at the Nevada Test Site: evaluation of vacuum removal of Pu-contaminated soil. *Health Phys* 1989;57(5):771–9.
- Shinn JH, Homan DN, Robinson WL. Resuspension studies in the Marshall Islands. *Health Phys* 1997;73:248–57.
- Toy TJ, Foster GR, Renard KG. *Soil erosion: processes, prediction, measurement and control*. New York: John Wiley & Sons, Inc.; 2002. 338 pp.
- Van Pelt, RS, Zobeck, TM. Chemical constituents of fugitive dust. In: Inyang H, Bae S, editors. *Special issue on particulate contaminant emissions from geomaterials*. *Environ Monit Assess* in press.
- Vogelmann JE, Sohl T, Howard SM. Regional characterization of land cover using multiple sources of data. *Photogramm Eng Remote Sensing* 1998;64:45–57.
- Wall BF, Hart D. Revised radiation doses for typical X-ray examinations. *Br J Radiol* 1997;70:437–9.
- Whicker FW, Shultz V. *Radioecology: nuclear energy and the environment*, vol. 2. Boca Raton: CRC Press; 1982. 228 pp.
- Whicker JJ, Breshears DD, Wasiolek PT, Kirchner TB, Tavani RA, Schoep DA, et al. Temporal and spatial variation of episodic wind erosion in unburned and burned semiarid shrubland. *J Environ Qual* 2002;31:599–612.
- Whicker FW, Hinton TG, MacDonell MM, Pinder III JE, Habegger LJ. Avoiding destructive remediation at DOE sites 2004. *Science* 2004;303:1615–6.
- Whicker JJ, Pinder JE, Breshears DD. Amplified wind erosion following forest thinning and burning. Los Alamos National Laboratory report LA-UR-05-0917; 2005.
- Whicker JJ, Pinder JE, Breshears DD. Increased wind erosion from wildfire: implications for contaminant-related risks. *J Environ Qual* 2006;35:468–78.
- Whitford WG, DeSoyza AG, Van Zee JW, Herrick JE, Havstad KM. Vegetation, soil, and animal indicators of rangeland health. *Environ Monit Assess* 1998;51:179–200.
- Zobeck TM, Fryrear DW, Pettit RD. Management effects on wind-eroded sediment and plant nutrients. *J Soil Water Conserv* 1989;44:160–3.